AIAA JOURNAL
Vol. 31, No. 2, February 1993

Mode Localization in Multispan Beams

S. D. Lust*
Hughes Aircraft Company, El Segundo, California 90245
and
P. P. Friedmann† and O. O. Bendiksen‡
University of California, Los Angeles, Los Angeles, California 90024

The influence of various effects on mode localization in multispan beams is studied. The finite element method is used to study localization as a function of Timoshenko beam effects; beam end conditions; span length, mass, and stiffness imperfection; viscous damping; axial force; transverse support and rotational coupling stiffness; and modeling resolution. Three configurations are studied, starting with two separate 2-span models and culminating in a 10-span configuration that resembles lattice-type large space structures. The results show that, in addition to the ratio of imperfection to coupling stiffness, transverse support stiffness and Timoshenko beam effects are also parameters that influence mode localization in structures with repeated segments.

Nomenclature

A = cross-sectional area
$\bar{A}$ = span response ratio
$[C]$ = damping matrix
c = continuous beam center support rotational spring stiffness
$\bar{c}$ = continuous beam center support nondimensional spring stiffness
E = Young's modulus of elasticity
G = shear modulus
I = mass moment of inertia
$[K]$ = stiffness matrix
K_r = pinned-beam rotational spring stiffness
$\overline{K_r}$ = pinned-beam rotational spring nondimensional stiffness
K_t = pinned-beam transverse spring stiffness
$\overline{K_t}$ = pinned-beam transverse spring nondimensional stiffness
k = shear correction factor
L = beam length (continuous beam) or span length (pinned beam)
L/r = slenderness ratio
$[M]$ = mass matrix
m = linear mass density
r = radius of gyration
$\{x\}$ = generalized coordinate vector
$\overline{\Delta E}$ = Young's modulus imperfection
ΔL = span length imperfection
$\overline{\Delta L}$ = nondimensional span length imperfection
λ = eigenvalue
ρ = mass density
Ω_n = natural frequency
$\overline{\Omega}_n$ = nondimensional natural frequency

Presented as Paper 90-1214 at the AIAA Dynamics Specialist Conference, Long Beach, CA, April 5-6, 1990; received May 10, 1991; revision received Sept. 7, 1992; accepted for publication Sept. 14, 1992.

*Senior Staff Engineer, Electro-Optical & Data Systems Group. Member AIAA.
†Professor, Mechanical, Aerospace, and Nuclear Engineering Department. Fellow AIAA.
‡Associate Professor, Mechanical, Aerospace, and Nuclear Engineering Department. Member AIAA.

I. Introduction and Problem Statement

WHEN modeling structures consisting of numerous repeated segments, structural dynamicists typically assume that the geometry and material properties (i.e., mass, stiffness, and damping) of the repeated elements are identical. The mode shapes obtained from this idealized model are global in nature, and the modal response extends throughout the structure.

However, in real structures, no two segments will be precisely identical. Imperfect manufacturing processes will invariably produce small random variations in the properties of each segment. These variations in segment properties are governed by manufacturing tolerances. If the ratio of segment variation to intersegment coupling falls within a certain range, the resultant mode shapes may be dramatically different from the idealized case. The modal response in this case is confined to a few segments or even a single segment of the structure, when compared with a conventional mode shape that extends throughout the structure. The degree and nature of the imperfections determine whether the localization is either beneficial, as a passive damping mechanism, or catastrophic, when it leads to excessive response or renders an active control system ineffective.

Early localization work in structural dynamics[1-9] dealt with the field of turbomachinery, which belongs to a class of cyclically symmetric structures that are weakly coupled and therefore susceptible to mode localization. The objective of this research was to explain the unpredicted fatigue failures of turbine and compressor blades. It is interesting to note that none of the early work on "mistuned" turbomachinery rotors mentions the term "mode localization." Reference 6 was among the first to use localization theory to explain the behavior of mistuned rotors.

The work of Bendiksen[10] and Cornwell and Bendiksen[11-13] focused primarily on the localization behavior of cyclically symmetric large space structures. In Ref. 10, the dynamic behavior for a perfectly symmetric wrap-rib antenna model was calculated by analytical methods. Numerical and perturbation methods were used to calculate localized modes for the disordered antenna model from the results of the perfect model analysis.[10] Multi-degree-of-freedom substructures were studied using Rayleigh-Ritz and finite element techniques.[11-13] The principal findings of this research determined 1) the sensitivities of eigenvalues and eigenvectors to small amounts of disorder and 2) the precise nature of coupling effects that cause localization. Time domain effects of localization were demonstrated by the confinement of a wave packet in the disordered structure, compared with the extended response of the tuned

structure. A method was also introduced to measure the extent of localization.

Hodges[14] studied mode localization from an acoustical viewpoint. Two models, a series of coupled pendulums and a vibrating string with point masses and springs, were used to show that the degree of localization was strongly influenced by the ratio of disorder strength to coupling strength. Using the vibrating string, Hodges and Woodhouse[15] demonstrated analytically and experimentally that vibration attenuation can be achieved by a random variation of the properties of a periodic structure.

Localization from a wave propagation perspective was studied by Kissel.[16] The structures considered in Ref. 16 consisted of a spring-mass chain and a rod carrying longitudinal waves with attached resonators. Kissel also defined a localization factor based on the spatial attenuation of the wave.

Work by Pierre[17] and Pierre et al.[18] studied localization for a two-span Bernoulli-Euler beam using analytical and experimental methods. Imperfection or disorder was achieved by perturbing the position of the center support from the midpoint of the beam. Variations in the coupling between the spans was introduced by modifying the stiffness of a center support rotational spring connecting the beam to ground. Analytical results were obtained by a modified perturbation method and a Rayleigh-Ritz technique. Localization curves were presented by plotting the span response ratios for each mode as functions of the length imperfection and the coupling parameter. The results agreed with Hodges[14] and Bendiksen,[10] indicating that the degree of localization depended on the ratio of disorder strength to coupling strength. Wei and Pierre[19,20] have also used perturbation methods to study localization in mistuned assemblies with cyclic symmetry.

Previous studies of beam structures[17,18] were based on Bernoulli-Euler beam theory. This approach led to a convenient solution that could be obtained in closed form or from convenient approximations such as the Rayleigh-Ritz technique and thus the computational effort could be minimized. However, when dealing with higher modes, wave propagation, or modeling truss or frame structures such as a continuum beam, the shear stiffness and rotatory inertia properties associated with Timoshenko beam theory become important and are required.[21] Closed-form Timoshenko beam eigensolutions exist only for the single-span case. However, it should be noted that exact dynamic stiffness matrices for Timoshenko beams have been derived in Refs. 22 and 23, and these can also be employed in the structural dynamic modeling of multispan beams. To analyze complex multispan beams, a finite element approach is needed. This approach, which is an essential ingredient for the study of large practical configurations, has not been considered in the literature to date.

The purpose of this study is to provide an improved fundamental understanding of mode localization phenomena in realistic multispan beam-type structures. To accomplish this objective, the following effects were studied: 1) modeling of shear stiffness and rotary inertia (Timoshenko beam effects) in the beam finite element model; 2) variation of boundary conditions such as clamped end conditions in addition to the simply supported case studied previously; 3) introduction of viscous damping; 4) variation of the number of elements per span in the Timoshenko beam finite element model, which effectively changes the relative spacing of bending and shear modes; 5) introduction of imperfection by variations in the span length, span mass, and span stiffness; 6) introduction of axial force effects; 7) variation of the center support transverse stiffness in addition to the rotational coupling stiffness; and 8) introduction of a discrete mass at an intermediate span location as an imperfection parameter. The numerical results presented in the paper illustrate in a clear manner the role of these parameters in mode localization.

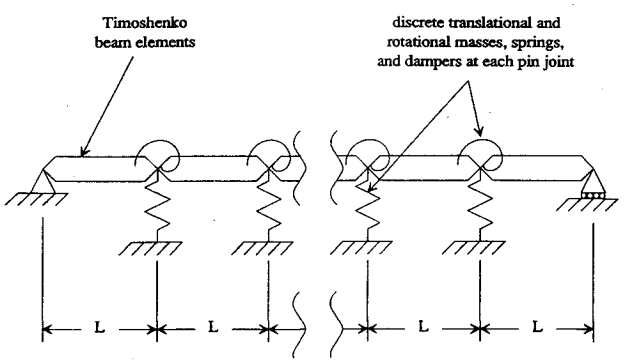

Fig. 1 General multispan beam-type structure.

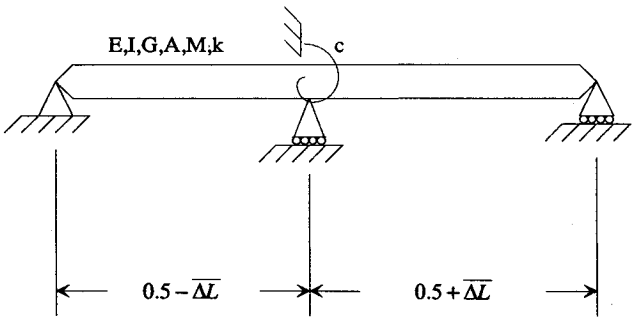

Fig. 2 Two-span continuous beam model.

II. Mathematical Model, Method of Solution, and Finite Element Code

A finite element model capable of representing general beam-type multispan configurations, including the effects of damping, Timoshenko beam effects, various degrees of coupling, and imperfection, was developed and implemented in a computer code.[24] The geometry for the model of the multispan beam is described in Fig. 1. Among the various available finite element models suitable for representing Timoshenko beams, the model developed by Tessler and Dong[25] was selected because it corrects many of the deficiencies present in other models. In Ref. 25, families of Timoshenko beams were developed with different orders of interpolation. From the family of elements available, the element denoted as T2CL6 was selected. This is a higher order element based on the concept of "interdependent variable interpolation" for the element formulation.[25] Details of the implementation of this element in the present formulation are presented in Refs. 26 and 27 and are not repeated here for the sake of conciseness.

The general beam configurations that can be represented by the finite element code that was developed, shown schematically in Fig. 1, consist of the T2CL6 Timoshenko beam element, combined with the capability for modeling axial loads, translational and rotational springs, masses, and viscous dampers. As shown in Fig. 1, each beam span is assumed to be pin connected to its neighbor. The code is capable of computing both damped and undamped free vibration problems.

For the undamped case, one has real, symmetric, and positive definite mass and stiffness matrices. The eigenvalues and mode shapes are obtained from solving the standard structural dynamics eigenvalue problem. In the program that was developed, Eq. (1) is solved by the EISPACK routine RSG[28]:

$$[K]\{x\} = \lambda[M]\{x\} \tag{1}$$

For the damped case, the equations are first rewritten in first order state variable form,[29] leading to the real, symmetric, nonpositive definite eigenvalue problem, Eq. (2), which is solved by EISPACK routine RGG:

$$\begin{bmatrix} [0] & [K] \\ [K] & [C] \end{bmatrix} \begin{Bmatrix} U \\ V \end{Bmatrix} = \lambda \begin{bmatrix} -[K] & [0] \\ [0] & [M] \end{bmatrix} \begin{Bmatrix} U \\ V \end{Bmatrix} \tag{2}$$

The output from the finite element program consists of the eigenvalues and eigenvectors, as well as strain and kinetic energies associated with the various modes. The kinetic energy is used as a device for identifying modes as predominantly shear or bending modes. A mode having greater transverse kinetic energy than rotational kinetic energy is defined as a bending mode. If the converse is true, the mode is defined as a shear mode.

III. Results and Discussion

Continuous Two-Span Beam

Studies to determine the influence of the Timoshenko beam effects on localization were conducted first. The example considered was a two-span beam studied by Pierre[17] and Pierre et al.[18] that is shown in Fig. 2. Natural frequencies Ω_n and span response ratios $\bar{A}$ were computed as functions of mode number, rotational stiffness at the center support c, and span length imperfection ΔL. The natural frequencies, rotational stiffnesses, and span length imperfections were represented by the nondimensional quantities given next:

$$\overline{\Omega_n} = \Omega_n / \sqrt{\frac{EI}{mL^4}} \tag{3}$$

$$\bar{c} = c\frac{2L}{EI} \tag{4}$$

$$\overline{\Delta L} = \frac{\Delta L}{L} \tag{5}$$

where L is the length of the entire beam.

The span response ratio $\bar{A}$ is illustrated in Fig. 3 and is defined as follows:

$$\bar{A} = \left|\frac{a}{b}\right| \tag{6}$$

where a is the maximum displacement associated with the span in which the response is smaller, and b is the maximum displacement associated with the span in which the response is larger.

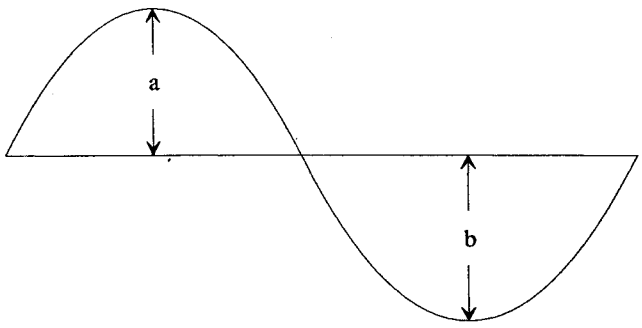

Fig. 3 Span response ratio.

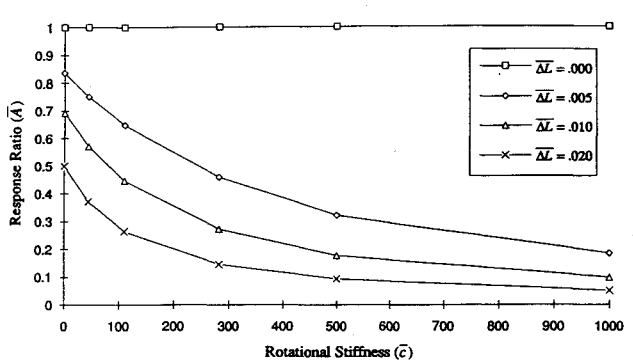

Fig. 4 Length imperfection localization curves, bending mode 6, Bernoulli-Euler elements.

Table 1 Bending mode natural frequencies of a perfect two-span continuous beam

Bending mode number	Beam element type			
	Bernoulli-Euler	T2CL6, $L/r = 55.4$	T2CL6, $L/r = 27.7$	T2CL6, $L/r = 10.1$
1	39.5	38.5	36.0	25.4
2	61.7	58.1	50.5	28.7
3	157.9	143.9	118.7	62.3
4	199.9	172.9	132.4	63.4
5	355.3	295.5	218.4	100.4
6	417.1	326.5	227.3	101.2
7	631.8	475.9	323.7	138.7
8	713.3	504.2	328.3	138.8
9	987.6	674.7	431.4	176.3
10	1088.9	698.5	431.7	176.6

Table 2 Shear mode natural frequencies of a perfect two-span continuous beam

Shear mode number	Beam element type			
	Bernoulli-Euler	T2CL6, $L/r = 55.4$	T2CL6, $L/r = 27.7$	T2CL6, $L/r = 10.1$
1	—	1735.5	433.9	57.4
2	—	1747.0	446.2	69.0
3	—	1780.6	476.3	89.1
4	—	1832.6	519.4	115.4

To facilitate comparison with the results obtained by Pierre[17] and Pierre et al.,[18] values for $\bar{c}$ were selected as 0.0, 44.8, 110.1, 281.8, 500.0, and 1000.0, respectively. Values for $\overline{\Delta L}$ were chosen as 0.0, 0.005, 0.010, and 0.020. Localization curves were obtained by plotting span response ratios $\bar{A}$ vs rotational stiffness $\bar{c}$ for constant values of length imperfection $\overline{\Delta L}$. To be consistent with Pierre's terminology, a mode is considered as "localized" when the span response ratio is less than 0.1.

Timoshenko Beam Effects

To study Timoshenko beam effects on mode localization, four cases were considered. The first case consisted of the continuous two-span beam modeled with Bernoulli-Euler elements. The remaining three cases modeled the two-span beam with T2CL6 elements. Slenderness ratios for the three Timoshenko beam examples were 55.4, 22.7, and 10.1, respectively.

Natural frequencies for the first 10 bending modes of the perfect structure ($\bar{c} = 0.0$ and $\overline{\Delta L} = 0.0$) are presented in Table 1. Natural frequencies for the first four shear modes of the perfect structure are given in Table 2. Inspection of the natural frequencies and their respective mode shapes reveals that the modes can be divided into pairs, which is expected since the example structure has two repeated segments. The Timoshenko beam effects manifest themselves by the decrease in bending mode natural frequencies. This effect becomes more pronounced with increasing mode number and decreasing slenderness ratio. The decrease in bending mode frequencies is also accompanied by a reduction in the frequency spacing associated with the mode pairs.

Shear mode natural frequencies also exhibit a significant decrease with decreasing slenderness ratio. However, the frequency spacing between mode pairs remains relatively small and nearly constant over the range of slenderness ratios.

Mode number 6 was selected to illustrate the results because it is the lowest bending mode for which the interaction between the bending and shear modes strongly influences localization for all of the slenderness ratios considered. Figures 4 and 5 present localization curves for bending mode 6 for the Bernoulli-Euler beam as well as for the T2CL6 beam with a

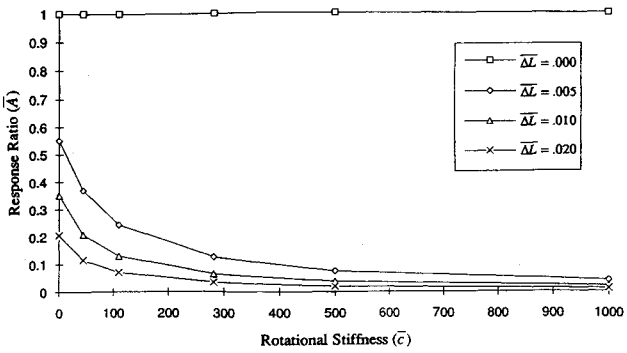

Fig. 5 Length imperfection localization curves, bending mode 6; T2CL6 elements $E/kG = 3.13$, $L/r = 27.7$.

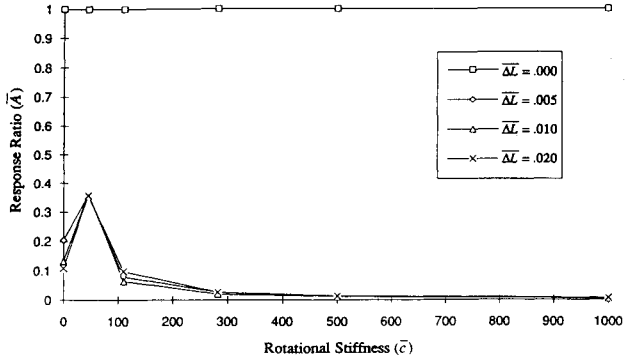

Fig. 6 Length imperfection localization curves, bending mode 6; T2CL6 elements $E/kG = 3.13$, $L/r = 10.1$.

slenderness ratio of 27.7. These curves represent typical localization behavior: localization increases with increasing rotational stiffness at the center support (decreased coupling), with increasing span length imperfection, and with increasing Timoshenko beam effects (decreasing slenderness ratio). In general, localization also increases with increasing mode number. This behavior of the localization curves agrees with previous research,[11,13] where it was shown that perfect structural systems with more closely spaced mode groups have a greater affinity for localization.

Delocalization is observed for the localization curves shown in Fig. 6 (mode 6, T2CL6 elements, $L/r = 10.1$). This delocalization, seen as an increase in the span response ratio for specific combinations of rotational stiffness $\bar{c}$ and length imperfection $\overline{\Delta L}$, is caused by the interaction of closely spaced bending and shear modes. Another type of delocalization occurs when the span length imperfection exceeds one-eighth of the mode shape wavelength.

Shear mode localization curves differ somewhat from bending mode curves. For bending modes, the span response ratio at $\bar{c} = 0.0$ is dependent on length imperfection and mode number. This dependence is particularly evident for higher order bending modes; localization is immediate when $\overline{\Delta L} > 0.0$. In contrast, shear mode localization curves approach a span response ratio of 1.0 at $\bar{c} = 0.0$ regardless of the mode number and length imperfection.

Beam End Conditions

The effects of beam end conditions on localization were determined analytically by using simply supported as well as clamped end conditions. At the center a simple support was retained for both cases. In general, span response ratios and, therefore, localization curve magnitudes for the fixed end conditions were approximately 95% of those for the simple supports. Thus, for the cases considered, the beam end conditions have little influence on localization for this particular configuration.

Damping

The influence of damping on the two-span beam configuration was also studied by introducing a rotational viscous damper at the center support. The computations were carried out for two different damping values, one representing nominal damping that can be encountered in a structure and the second representing high values of damping. The rotational damper was tuned to yield approximately 1 and 10% critical damping, respectively, for mode 1. Span response ratios for both damped configurations were virtually identical with those of the undamped system. This implies that localization is a fairly robust phenomenon, which is unaffected by the presence of damping.

It should also be noted that damping in a multispan beam (having more than two spans) could be added in an imperfect manner, and then its influence would be similar to any other imperfection. The results from the two-span beam indicate that such calculations would not be productive.

Pinned Two-Span Beam

Additional studies on the two-span beam configuration, depicted in Fig. 7, were conducted. The objective was to demonstrate the sensitivity of localization to changes in center support location (span length), mass, stiffness, axial force, and center support stiffness. This two-span beam differs from the structure considered in the previous example because 1) the spans are connected by a pin joint, rather than the beam being continuous; 2) the spans are coupled at the pin joint by a rotational spring K_r; and 3) in some cases, the simple support at the center is replaced by a transverse spring K_t. These changes transform the configuration shown in Fig. 2 into a much more practical configuration that resembles a building block that may be encountered in a multispan large space structure.

The rotational and transverse springs were nondimensionalized with respect to EI/L and EI/L^3, respectively, for the beam. Therefore, the nondimensional values for $\overline{K_r}$ and $\overline{K_t}$ are defined by the following relations:

$$\overline{K_r} = \frac{K_r L}{EI} \tag{7}$$

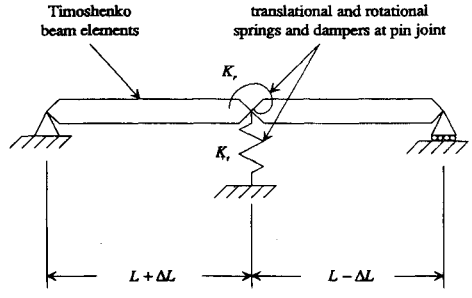

Fig. 7 Two-span pinned-beam model.

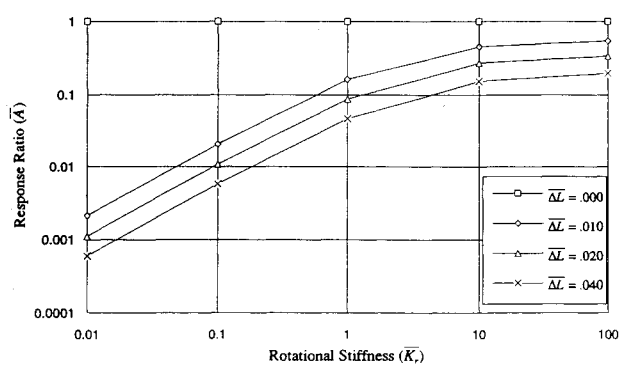

Fig. 8 Length imperfection localization curves, bending mode 6; T2CL6 elements $E/kG = 3.13$, $L/r = 13.9$.

$$\overline{K_t} = \frac{K_t L^3}{EI} \tag{8}$$

where L is the nominal length of the individual spans.

Span Length Imperfection

For the first two cases calculated for the pinned two-span beam, natural frequencies and response ratios were obtained and plotted as functions of span length imperfection and rotational spring coupling. Two values of slenderness ratio were considered: $L/r = 13.9$ and 27.7, respectively. For a slenderness ratio of $L/r = 13.9$, a localization curve plot for bending mode 6 is shown in Fig. 8. Note that the shape of the curve is different from continuous two-span beam results because the nature of the span coupling is now different. For the continuous beam structure, increasing the rotational spring at the center support decreased coupling. For the pinned spans, increased spring stiffness increases coupling.

Examination of the localization curves reveals that length imperfection in the pinned two-span beam produces similar behavior to that observed in the continuous two-span beam.

Mass and Stiffness Imperfection

The effects of mass imperfection were studied by increasing the material density ρ of one of the spans by 0.5, 1, and 2%; thus the span mass and rotational inertia were increased by equal amounts. Bending and shear stiffness imperfections were introduced by increasing Young's modulus E for one of the spans by 0.5, 1, and 2%. These imperfections cause the same localization effects as length changes, but to a lesser degree. As evident from Fig. 9, the stiffness imperfection localization curves for bending mode 6 have the same trends as those for length imperfection (Fig. 8). However, localization associated with length imperfection is much more dramatic, when the same magnitudes of imperfection are considered. No difference was observed in the localization curves when comparing mass and stiffness imperfections. Equal changes in mass and stiffness yield equal and opposite changes in natural frequency. Mode shapes are modified such that the spans localize in opposite order.

Axial Force

The sensitivity of localization to axial force effects was also studied by applying varying levels of axial force to a pinned two-span beam with a 1.0% length imperfection. The critical buckling load for the beam was calculated, and compressive axial loads corresponding to 0, 60, 90, and 96% of the critical load were applied to the beam. The natural frequencies and span response ratios in the presence of these axial loads were computed. The results indicate that compressive axial loads have only a slight delocalizing effect on the beam behavior.[27]

Center Support Transverse Stiffness

All previous computations were done with a simple support at the center of the two-span beam configuration. In practice,

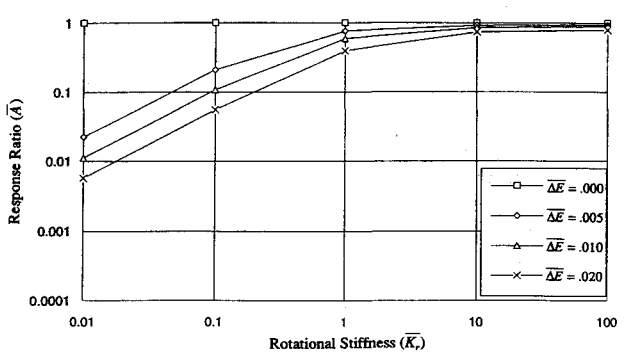

Fig. 9 Stiffness imperfection localization curves, bending mode 6; T2CL6 elements $E/kG = 3.13$, $L/r = 13.9$.

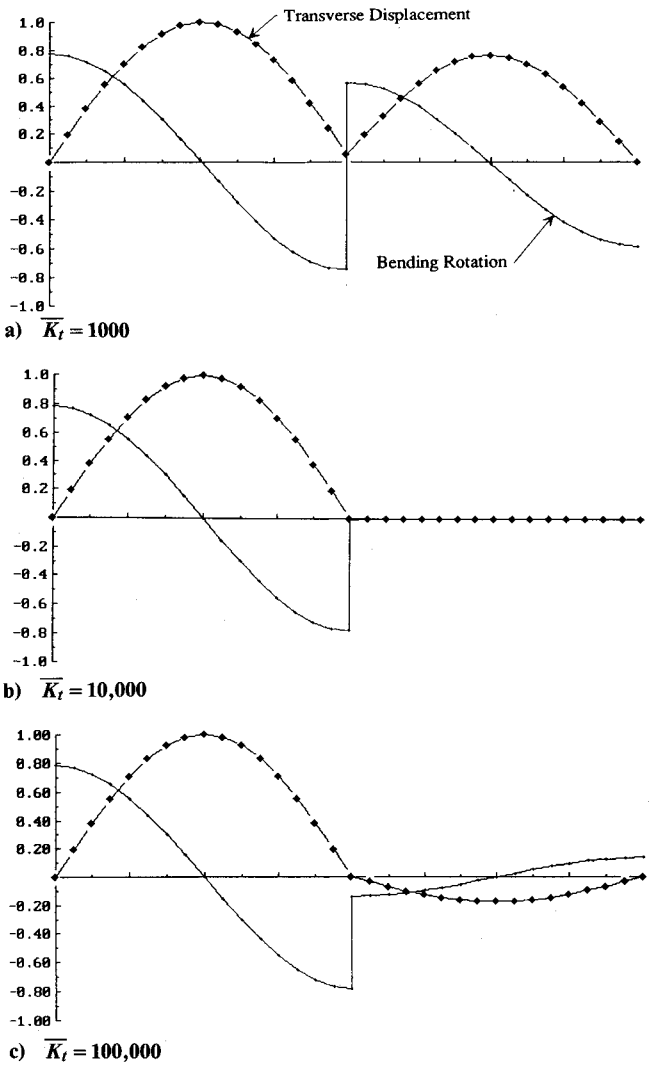

Fig. 10 Two-span pinned-beam, mode shape 1, $\overline{\Delta E} = 0.01$, $\overline{K_r} = 0.01$.

infinitely stiff supports do not exist. Therefore, the simple support was replaced with a transverse spring. Nondimensional values for the transverse spring $\overline{K_t}$ were varied from 100 to 100,000 by factors of 10. Since the beam transverse stiffness coefficient is $12EI/L^3$, these values of $\overline{K_t}$ range from approximately 100 to 10,000 times the beam transverse stiffness. As a limiting case, infinite transverse stiffness was represented by the simple support. Coupling stiffness $\overline{K_r}$ was varied from 0.01 to 100, corresponding to rotational coupling on the order of 300 times less to 30 times greater than the beam bending stiffness. Imperfection was introduced by varying Young's modulus E by 1%.

The localization curves for this case show an interesting phenomenon: first localization, followed by delocalization, occurs as the transverse support stiffness is increased. The magnitude of transverse stiffness at which the smallest span response ratio occurs is a function of the coupling stiffness $\overline{K_r}$ and the mode number. Once the coupling stiffness has attained a value of 10 or more, no significant localization effects are seen.

An explanation for localization and delocalization in the two-span structure can be gleaned from examining the mode shapes. Figures 10a–10c show plots of mode shape 1, with a coupling stiffness of 0.01 and increasing values of transverse spring stiffness from 1000 to 100,000. (Transverse displacement is represented by curves with the diamond pattern. Bending rotation is represented by the unmarked curves.) As the transverse spring stiffness is increased, the mode shape makes a transition from one shape to another. During the transition,

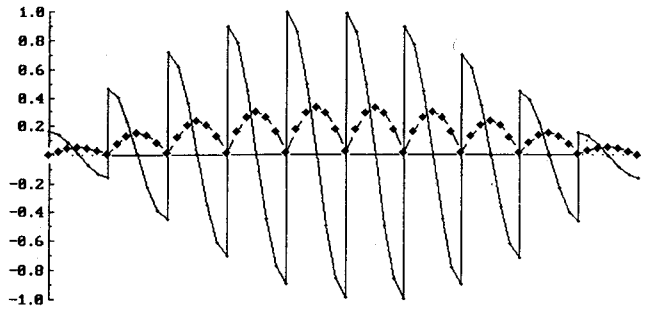

a) $\overline{K_t} = 1000$

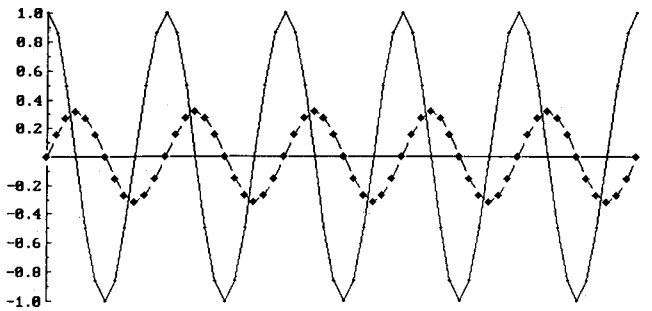

b) $\overline{K_t} = 10{,}000$

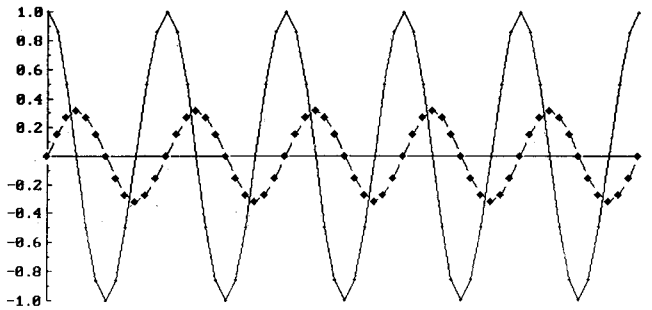

c) $\overline{K_t} = 100{,}000$

Fig. 11 Perfect 10-span beam, mode shape 1, $\overline{K_r} = 0.01$.

the superposition of the two shapes causes cancellation of the response for one span.

For a coupling stiffness value of 0.1, the shape transition occurs at a lower value of transverse spring stiffness and over a smaller interval of stiffness change. Increasing the coupling stiffness to 1.0 or 10.0 results in complete mode shape transition within the order of magnitude change of transverse spring stiffness. It is not clear whether any localization occurs within these small transition regions, and analyses with finer transverse stiffness resolution are needed to resolve this question.

Pinned 10-Span Beam

A 10-span version of the pinned 2-span example beam is considered next. The 10-span beam is a more realistic example, having some of the features that may be encountered in repetitive large space structures. The purpose of the 10-span beam analyses is to examine in a more comprehensive manner the localization/delocalization phenomena observed in the 2-span beam. In addition, cases were also computed to determine the effects of discrete masses that are added at the midpoint of selected spans of an otherwise perfect system.

To maintain similarity with the 2-span beam configuration, the 10-span version has simple supports at the ends and transverse springs at the intermediate joints. The range of values for the transverse spring stiffness $\overline{K_t}$ and coupling spring stiffness $\overline{K_r}$ were the same as for the 2-span cases. Transverse support springs and rotational coupling springs were varied in conjunction and not individually.

A slenderness ratio of 144.3 was chosen for the T2CL6 elements. The large slenderness ratio diminishes the shear and rotatory inertia effects associated with the Timoshenko beam formulation. Therefore the results obtained are indicative of both Timoshenko and Bernoulli-Euler beam behavior.

Transverse Support Stiffness

As a starting point for investigating the behavior of disordered systems, analyses were performed for the perfect system over the range of $\overline{K_t}$ and $\overline{K_r}$ values. Imperfection was then introduced by a random variation in the value of Young's modulus E for the spans. A Gaussian distribution of moduli was chosen such that 95% of the values would fall within 2% of the nominal value. For the 10-span problem, the random distribution generated moduli from -0.79 to $+1.11$% of the nominal. Bending and shear stiffness properties for each span were calculated from the random representation of Young's moduli. The analyses for the range of $\overline{K_r}$ and $\overline{K_t}$ values were then repeated for this disordered system.

Localization behavior for mode 1 of the perfect and imperfect 10-span models are shown in Figs. 11a–12c. Figures 11a–11c present perfect structure mode shapes, whereas Figs. 12a–12c present corresponding mode shapes for the imperfect structure. The mode shape plots represent stiffness values of $\overline{K_r} = 0.01$ and $\overline{K_t}$ ranging from 1000 to 100,000. Mode shapes for the perfect structure are extended for all cases. For the imperfect structure, complete localization occurs for $\overline{K_t} = 10{,}000$ in Fig. 12b, with slight delocalization seen for $\overline{K_t} = 100{,}000$ in Fig. 12c.

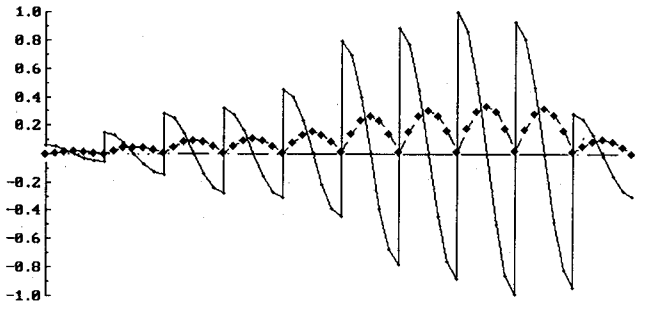

a) $\overline{K_t} = 1000$

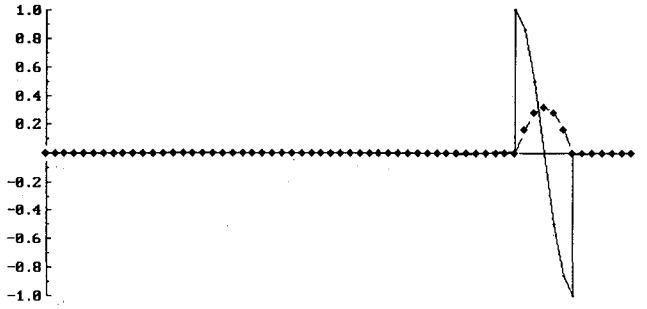

b) $\overline{K_t} = 10{,}000$

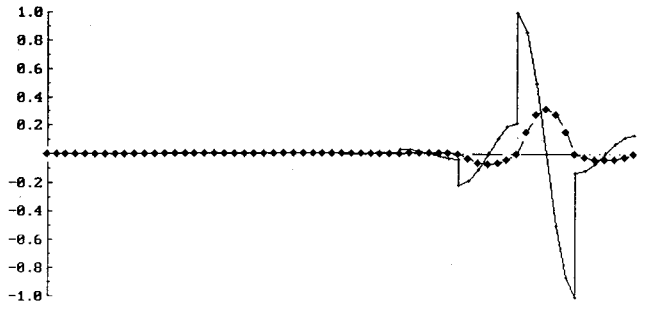

c) $\overline{K_t} = 100{,}000$

Fig. 12 Imperfect 10-span beam, mode shape 1, $\overline{K_r} = 0.01$.

When the coupling stiffness $\overline{K_r}$ is increased to 0.1, localization is not as complete as for the more weakly coupled system, but it is still quite evident. Delocalization, however, is much more dramatic. Significant response levels are present throughout the structure. Figures 13a–14c present the comparison of the perfect and imperfect structures for $\overline{K_t} = 0.1$ and $\overline{K_r}$ ranging from 100 to 10,000.

For coupling stiffnesses of 1.0 and 10.0, the imperfect system mode shapes closely approximate those of the perfect system. No localization is evident in the mode shapes, but as in the case of the two-span beam, analyses with a finer resolution for $\overline{K_t}$ are required to determine dynamic behavior in the transition region. From these results it is evident that the most interesting localization effects occur in multispan structures, which have many repetitive elements.

Discrete Mass Imperfection

Discrete masses equal to 1% of the span weight were sequentially added at the midpoint of spans 4, 8, and 6 of the perfect structure. Analyses were then performed for each of these cases for the range of transverse and rotational stiffnesses previously noted. Spans with the added masses experienced localized responses for the same combinations of $\overline{K_t}$ and $\overline{K_r}$ that produced localized modes for the imperfect structure with random Young's moduli.

These results seem to indicate that small concentrated masses could be used to control localization. Given a structure with known localized modes, it might be possible to add such discrete masses as a means of transforming localized modes to extended modes. Conversely, given a perfect structure, discrete masses may be added to create localized modes and therefore inhibit the propagation of response through the structure.

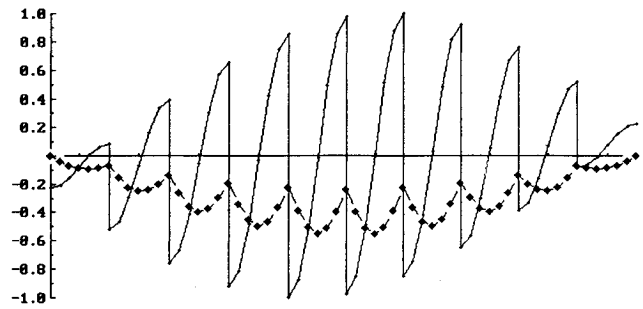

a) $\overline{K_t} = 100$

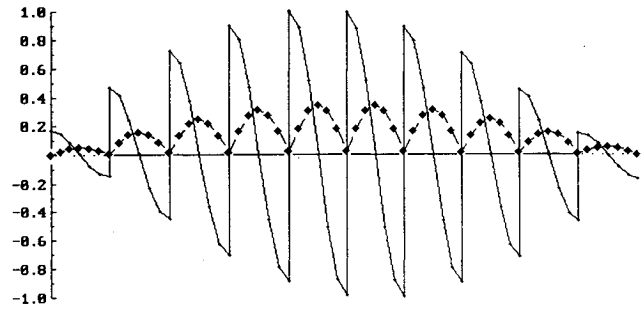

b) $\overline{K_t} = 1000$

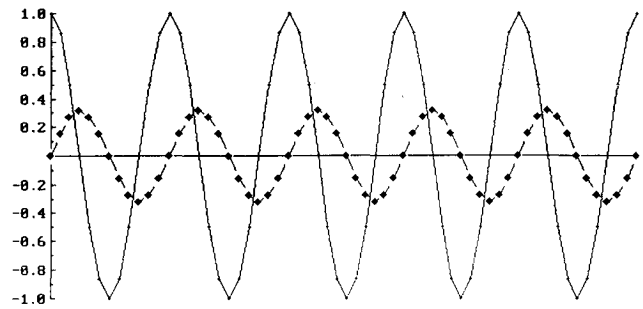

c) $\overline{K_t} = 10{,}000$

Fig. 13 Perfect 10-span beam, mode shape 1, $\overline{K_r} = 0.1$.

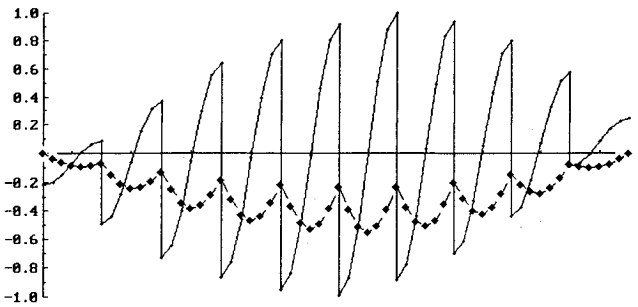

a) $\overline{K_t} = 100$

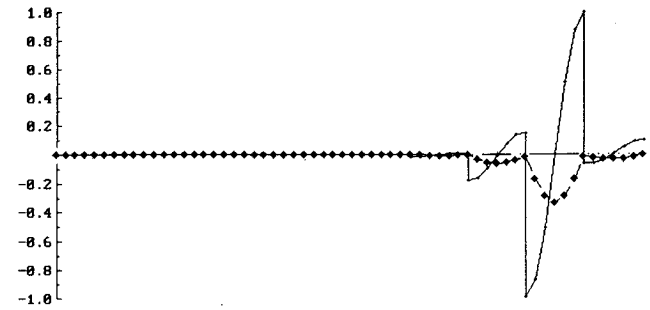

b) $\overline{K_t} = 1000$

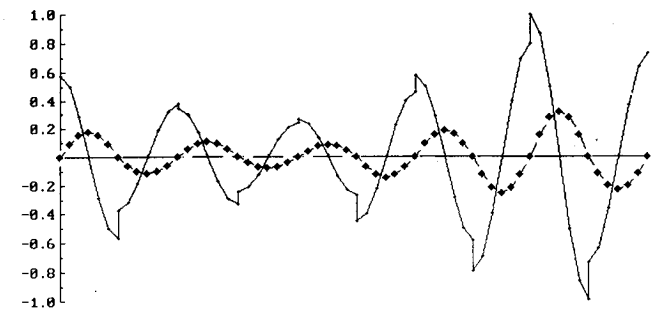

c) $\overline{K_t} = 10{,}000$

Fig. 14 Imperfect 10-span beam, mode shape 1, $\overline{K_r} = 0.1$.

IV. Concluding Remarks

A summary of the more important conclusions obtained in the course of this study are presented here.

1) The Timoshenko beam formulation has a significant influence on localization for higher modes, especially in the range where bending-shear mode interaction occurs.

2) Span length imperfection causes increased localization when compared with mass or stiffness imperfection of the same magnitude.

3) For a multispan pinned-beam configuration, a nondimensional rotational coupling stiffness of 10 or greater effectively prevents localization for physically "reasonable" values of imperfection.

4) Transverse span support stiffness is extremely important for nondimensional rotational coupling stiffness of less than 1.

5) For the two-span model, neither axial load nor rotational viscous damping at the center support is an important localization parameter.

6) A new and important phenomenon, delocalization, has been observed for the first time in this study. This phenomenon is influenced by three separate ingredients that can act either independently or in conjunction with each other. These ingredients are 1) interaction of bending and shear modes, 2) beam length imperfections that exceed one-eighth of the mode shape wavelength, and 3) the influence of transverse support stiffness.

The conclusions just presented are based exclusively on the behavior of the eigenvalues and eigenvectors computed for the structural dynamic system. However, the response to continuous or impulsive loads should also be calculated to obtain an improved understanding of the relative influence of parameters affecting localization. These effects have also been studied in Refs. 27 and 30 and will be presented in a sequel to this paper.

Acknowledgments

This research was funded by the Jet Propulsion Laboratory, Pasadena, CA, under Contract 958410, with M. Salama as monitor. His useful comments and support are hereby gratefully acknowledged.

References

[1]Dye, R. C. F., and Henry, T. A., "Vibration Amplitudes of Compressor Blades Resulting from Scatter in Blade Natural Frequencies," *ASME, Journal of Engineering for Power,* Vol. 91, No. 7, 1969, pp. 182–188.

[2]El-Bayoumy, L. E., and Srinivasan, A. V., "Influence of Mistuning on Rotor-Blade Vibrations," *AIAA Journal,* Vol. 13, No. 4, 1975, pp. 460–464.

[3]Ewins, D. J., "Vibration Modes of Mistuned Bladed Disks," *ASME, Journal of Engineering for Power,* Vol. 98, No. 7, 1976, pp. 349–355.

[4]Kaza, K. R. V., and Kielb, R. E., "Flutter and Response of a Mistuned Cascade in Incompressible Flow," *AIAA Journal,* Vol. 20, No. 8, 1982, pp. 1120–1127.

[5]Bendiksen, O. O., "Flutter of Mistuned Turbomachinery Rotors," *ASME, Journal of Engineering for Gas Turbines and Power,* Vol. 106, No. 1, 1984, pp. 25–33.

[6]Bendiksen, O. O., "Aeroelastic Stabilization by Disorder and Imperfections," Paper 583P, 16th IUTAM Congress of Theoretical and Applied Mechanics, Lyngby, Denmark, Aug. 1984.

[7]Kaza, K. R. V., and Kielb, R. E., "Flutter of Turbofan Rotors with Mistuned Blades," *AIAA Journal,* Vol. 22, No. 11, 1984, pp. 1618–1625.

[8]Valero, N. A., and Bendiksen, O. O., "Vibration Characteristics of Mistuned Shrouded Blade Assemblies," *ASME, Journal of Engineering for Gas Turbines and Power,* Vol. 108, No. 4, 1986, pp. 293–299.

[9]Bendiksen, O. O., and Valero, N. A., "Localization of Natural Modes of Vibration in Bladed Disks," ASME Paper 87-GT-46, American Society of Mechanical Engineers, New York, June 1987.

[10]Bendiksen, O. O., "Mode Localization Phenomena in Large Space Structures," *Proceedings of the 27th AIAA/ASME/ASCE/AHS Structures, Structural Dynamics, and Materials Conference* (San Antonio, TX), AIAA, New York, May 19–21, 1986, pp. 325–335 (AIAA Paper 86-0903).

[11]Cornwell, P. J., and Bendiksen, O. O., "Localization of Vibrations in Large Space Reflectors," *Proceedings of the 28th AIAA/ASME/ASCE/AHS Structures, Structural Dynamics, and Materials Conference* (Monterey, CA), AIAA, New York, April 6–8, 1987, pp. 925–935 (AIAA Paper 87-0949).

[12]Cornwell, P. J., and Bendiksen, O. O., "Forced Vibrations in Large Space Reflectors with Localized Modes," *Proceedings of the 30th AIAA/ASME/ASCE/AHS Structures, Structural Dynamics, and Materials Conference* (Mobile, AL), AIAA, Washington, DC, April 3–5, 1989, pp. 188–198 (AIAA Paper 89-1180).

[13]Cornwell, P. J., and Bendiksen, O. O., "A Numerical Study of Vibration Localization in Disordered Cyclic Structures," *Proceedings of the 30th AIAA/ASME/ASCE/AHS Structures, Structural Dynamics, and Materials Conference* (Mobile, AL), AIAA, Washington, DC, April 3–5, 1989, pp. 199–208 (AIAA Paper 89-1181).

[14]Hodges, C. H., "Confinement of Vibration by Structural Irregularity," *Journal of Sound and Vibration,* Vol. 82, No. 3, 1982, pp. 411–424.

[15]Hodges, C. H., and Woodhouse, J., "Vibration Isolation from Irregularity in a Nearly Periodic Structure: Theory and Measurements," *Journal of the Acoustical Society of America,* Vol. 74, No. 3, 1983, pp. 894–905.

[16]Kissel, G. J., "Localization in Disordered Periodic Structures," *Proceedings of the 28th AIAA/ASME/ASCE/AHS Structures, Structural Dynamics, and Materials Conference* (Monterey, CA), AIAA, New York, April 6–8, 1987, pp. 1046–1055 (AIAA Paper 87-0819).

[17]Pierre, C., "Analysis of Structural Systems with Parameter Uncertainties," Ph.D. Dissertation, Duke Univ., Durham, NC, 1985.

[18]Pierre, C., Tang, D. M., and Dowell, E. H., "Localized Vibrations of Disordered Multi-Span Beams: Theory and Experiment," *Proceedings of the 27th AIAA/ASME/ASCE/AHS Structures, Structural Dynamics, and Materials Conference* (San Antonio, TX), AIAA, New York, May 19–21, 1986, pp. 445–455 (AIAA Paper 86-0934).

[19]Wei, S.-T., and Pierre, C., "Localization Phenomena in Mistuned Assemblies with Cyclic Symmetry, Part I: Free Vibrations," *Journal of Vibration, Acoustics, Stress, and Reliability in Design,* Vol. 110, No. 10, 1988, pp. 429–438.

[20]Wei, S.-T., and Pierre, C., "Localization Phenomena in Mistuned Assemblies with Cyclic Symmetry, Part II: Forced Vibrations," *Journal of Vibration, Acoustics, Stress, and Reliability in Design,* Vol. 110, No. 10, 1988, pp. 439–449.

[21]Magrab, E. A., *Vibrations of Elastic Structural Members,* Sijthoff & Noordhoff, Alpen aan den Rijn, The Netherlands, 1979, pp. 93–214.

[22]Henshell, R. D., and Warburton, G. B., "Transmission of Vibration in Beam Systems," *International Journal for Numerical Methods in Engineering,* Vol. 1, 1969, pp. 47–66.

[23]Howson, W. P., and Williams, F. W., "Natural Frequencies of Frames with Axially Loaded Timoshenko Members," *Journal of Sound and Vibration,* Vol. 26, No. 4, 1973, pp. 503–515.

[24]Hinton, E., and Owen, D. R. J., *Finite Element Programming,* Academic Press, New York, 1977, pp. 47-94.

[25]Tessler, A., and Dong, S. B., "On a Hierarchy of Conforming Timoshenko Beam Elements," *Computers & Structures,* Vol. 14, No. 3-4, 1981, pp. 335–344.

[26]Lust, S. D., Friedmann, P. P., and Bendiksen, O. O., "Mode Localization in Multi-Span Beams," *Proceedings of the AIAA Dynamics Specialist Conference* (Long Beach, CA), AIAA, Washington, DC, April 5–6, 1990, pp. 225–235 (AIAA Paper 90-1214-CP).

[27]Lust, S. D., "Free and Forced Response of Nearly Periodic Multi-Span Beams and Multi-Bay Trusses," Ph.D. Dissertation, Univ. of California, Los Angeles, Los Angeles, CA, 1991.

[28]Garbow, B. S., Boyle, J. M., Dongarra, J. J., and Moler, C. B., *Matrix Eigensystem Routines—EISPACK Guide Extension,* Springer-Verlag, Berlin, 1977, pp. 186–313.

[29]Dong, S. B., and Demsetz, S. S., "Eigenvector Relations for Natural Vibrations of Damped Systems," *Proceedings of the 1985 SAE Aerospace Technology Conference and Exposition* (Long Beach, CA), SAE Special Publication SP-635, Society of Automotive Engineers, Warrendale, PA, Oct. 14–17, 1985, pp. 55–59 (SAE Paper 851931).

[30]Lust, S. D., Friedmann, P. P., and Bendiksen, O. O., "Free and Forced Response of Nearly Periodic Multi-Span Beams and Multi-Bay Trusses," *Proceedings of the 32nd AIAA/ASME/ASCE/AHS/ASC Structures, Structural Dynamics, and Materials Conference* (Baltimore, MD), AIAA, Washington, DC, April 8–10, 1991, pp. 2831–2842 (AIAA Paper 91-0999-CP).